Science Advances
AAAS

Supplementary Materials for

Unconditional Fock state generation using arbitrarily weak photonic nonlinearities

Andrew Lingenfelter*, David Roberts, A. A. Clerk

*Corresponding author. Email: lingenfelter@uchicago.edu

Published 26 November 2021, *Sci. Adv.* **7**, eabj1916 (2021)
DOI: 10.1126/sciadv.abj1916

This PDF file includes:

I Multi-mode generalization and preparation of non-Gaussian entangled states

Our basic scheme in Eq. (1) can be easily extended to a mechanism that allows the generation of entangled M-mode non-Gaussian photonic states *using only weak nonlinearities* $U \ll \kappa$. For concreteness, we describe here the extension to a $M = 2$ mode system with lowering operators $\hat{a}_1, \hat{a}_2$. The idea is simple: we again want to realize the nonlinear driving Hamiltonian in Eq. (1) in a displaced frame, but now the single-mode lowering operator $\hat{a}$ by a collective mode, e.g.

$$\hat{b} = (\hat{a}_1 + \hat{a}_2)/\sqrt{2}. \tag{S1.1}$$

The desired nonlinear driving Hamiltonian is

$$\hat{H}_{\text{block},2} = \tilde{\Lambda}\hat{b}^\dagger(\hat{b}^\dagger\hat{b} - r) + \text{h.c.}. \tag{S1.2}$$

In what follows, we focus on realizing a single-excitation state, and hence take $r = 1$. Following the logic of "Dynamics for ideal drive amplitude matching", the ideal dynamics under this Hamiltonian can prepare a single excitation in the collective b mode. If we use the photon number of each a_1, a_2 mode to separately encode a qubit, than the single excitation state produced is a maximally entangled Bell state $(|10\rangle + |01\rangle)/\sqrt{2}$.

We stress that the Hamiltonian in Eq. (S1.2) amounts to simply replacing $\hat{a}$ in Eq. (1) of the main text with the collective mode $\hat{b}$. It thus immediately follows that if we take the four-wave mixing Hamiltonian Eq. (2) in the main text, replace $\hat{a}$ with $\hat{b}$, then the resulting Hamiltonian is equivalent to Eq. (S1.2) up to unitary displacement operators of modes $\hat{a}_1$ and $\hat{a}_2$.

Given this, a simple substitution then in Eq. (2) yields the required form of the starting two-mode Hamiltonian

$$\hat{H}_{\text{RWA},2} = U\hat{b}^\dagger\hat{b}^\dagger\hat{b}\hat{b} + \Delta\hat{b}^\dagger\hat{b} + (\Lambda_1\hat{b}^\dagger + \Lambda_2\hat{b}^\dagger\hat{b}^\dagger + \text{h.c.}). \tag{S1.3}$$

where again $\hat{b}$ is given by Eq. (S1.1). The linear and quadratic terms that are generated describe linear drives on both modes, detuning and beam-splitter couplings, and parametric drives (both degenerate and non-degenerate). The nonlinear four-wave mixing terms take the form

$$\hat{H}_{\text{RWA},2,U} = \frac{U}{2}\left(\sum_{j,k=1}^{2}\hat{a}_j^\dagger\hat{a}_k^\dagger\hat{a}_j\hat{a}_k + \left(\hat{a}_1^\dagger\hat{a}_1^\dagger\hat{a}_2\hat{a}_2 + \text{h.c.}\right)\right) \tag{S1.4}$$

Note that we now require both self and cross Kerr interactions, but also four-wave mixing processes that exchange interactions between modes 1 and 2.

Following the logic of the main text, we imagine displacing each mode $\hat{a}_j$ by the amplitude α_b given in Eq. (4). By further tuning the parameters the drive parameters Λ_1, Λ_2 and detuning parameter Δ as per Eqs. (5), the above two-mode Hamiltonian is unitarily equivalent to the desired two-mode blockade Hamiltonian in Eq. (S1.2). We thus show how our basic ideas generalize directly to multi-mode systems; other related approaches are also possible. While the introduction of modes does involve more complexities, the basic feature of our original scheme remains: generation of non-classical blockaded (now entangled) states is possible even if the four-wave mixing nonlinearities U are much weaker that photonic loss.

II Displacement error modeling and discussion of phase noise

The protocol for generating single photons (see Fig. 5) requires a rapid displacement of the cavity by an amplitude α_b (see Eq. (4)) at the beginning and a rapid displacement by $-\alpha_b$ at the end of the protocol. These displacements will not be perfect in any experiment so we must model small errors in them. Instead of enumerating specific possible errors that can occur during the displacements, we elected to offer a general error model via the Gaussian additive thermal noise channel. The thermal noise model not only provides results on how the correlation function $g^{(2)}(0)$ is bounded by the initial thermal occupation of the cavity, it can also be directly connected to errors in the displacement parameter α_b. As we show, this model also allows one to directly assess the impact of classical displacement noise. We also discuss how an almost identical approach can be used to model classical phase noise.

Displacement errors occur when the displacement amplitude is not α_b but some

$$\tilde{\alpha}_b = \alpha_b + \delta \tag{S2.1}$$

for some small complex error δ. We treat these errors generally by letting δ be a complex zero-mean Gaussian random variable with variance σ^2. Averaging over these random displacements starting from vacuum $|0\rangle$ results in a thermal state [30]; or in our case, a thermal state displaced by α_b. The occupation number $\bar{n}_{\mathrm{th}}$ of the thermal state is related to the variance σ^2 of the random displacement errors by

$$\bar{n}_{\mathrm{th}} = \sigma^2. \tag{S2.2}$$

One can see this by comparing the variance of the cavity quadratures for the thermal state and for the Gaussian average of the displaced coherent states. To model the displacement errors during the initial displacement numerically, we perfectly displace a thermal state with some occupation $\bar{n}_{\mathrm{th}}$:

$$|0\rangle\langle 0| \mapsto \hat{D}(\alpha_b)\hat{\rho}_{\mathrm{th}}(\bar{n}_{\mathrm{th}})\hat{D}^\dagger(\alpha_b) \tag{S2.3}$$

where $\hat{D}$ is the displacement operator.

At the end of the protocol we must displace the cavity back to the origin and apply the thermal noise channel. Applying the thermal noise channel to the blockaded state is not so easy because it is no longer a coherent state. Fortunately we are not particularly interested in the exact form of the final state, we are only interested in the correlation functions $\langle\hat{a}^\dagger\hat{a}\rangle$ and $\langle\hat{a}^\dagger\hat{a}^\dagger\hat{a}\hat{a}\rangle$ as these are all we need to compute $g^{(2)}(0)$. Thus at the end of the protocol, we perform a perfect displacement $-\alpha_b$, then we inject the same thermal noise into the final state by passing the cavity mode $\hat{a}$ through a beamsplitter with transmissivity $1-\epsilon$. A mode $\hat{b}$ with a thermal state, occupation $\langle \hat{b}^\dagger \hat{b} \rangle = \tilde{n}$, is put on the vacuum port of the beamsplitter. The output mode is thus

$$\hat{c} = \sqrt{1-\epsilon}\hat{a} + \sqrt{\epsilon}\hat{b}. \tag{S2.4}$$

We will consider the limit $\epsilon \to 0$, $\tilde{n} \to \infty$ such that $\epsilon\tilde{n} = \bar{n}_{\rm th}$ is fixed. Now assuming $\langle \hat{a} \rangle = 0$, a reasonable assumption as the coherence between $|0\rangle$ and $|1\rangle$ decays very quickly during the protocol, we find

$$\langle \hat{c}^\dagger \hat{c} \rangle = \langle \hat{a}^\dagger \hat{a} \rangle + \bar{n}_{\rm th}, \tag{S2.5}$$

$$\langle \hat{c}^\dagger \hat{c}^\dagger \hat{c}\hat{c} \rangle = \langle \hat{a}^\dagger \hat{a}^\dagger \hat{a}\hat{a} \rangle + 4\langle \hat{a}^\dagger \hat{a} \rangle \bar{n}_{\rm th} + 2\bar{n}_{\rm th}^2, \tag{S2.6}$$

after taking the limit $\epsilon \to 0$, $\tilde{n} \to \infty$. Finally for small $\bar{n}_{\rm th} \ll \langle \hat{a}^\dagger \hat{a} \rangle$, we compute $g^{(2)}(0) = \langle \hat{c}^\dagger \hat{c}^\dagger \hat{c}\hat{c} \rangle / \langle \hat{c}^\dagger \hat{c} \rangle^2$ to place the bound

$$g^{(2)}(0) \geq \frac{\langle \hat{a}^\dagger \hat{a}^\dagger \hat{a}\hat{a} \rangle}{\langle \hat{a}^\dagger \hat{a} \rangle^2} + \frac{4\bar{n}_{\rm th}}{\langle \hat{a}^\dagger \hat{a} \rangle}. \tag{S2.7}$$

In the numerical simulations, we perform a perfect displacement back to the origin at the end of the protocol and use this expression to bound $g^{(2)}(0)$.

The Gaussian thermal noise model as presented above describes the additive noise of small displacement errors $\tilde{\alpha}_b = \alpha_b + \delta$. The results presented in Fig. 1 of the main text are thus readily interpreted as additive displacement errors via Eq. (S2.2). Already this allows an experimentalist to determine the maximum allowed fractional error of the displacements to achieve a desired $g^{(2)}(0)$. Of course, with all other parameters fixed, this maximum fractional error is dependent on the displacement α_b.

In some experimental settings, a more natural error model would correspond to the noise-corrupted displacement having the form

$$\tilde{\alpha}_b = (1+\delta)\alpha_b. \tag{S2.8}$$

This could arise, e.g., because the coherent tone source, e.g., optical laser or microwave generator, will have a limited precision to which its output power and phase can be controlled. Again if δ is a complex Gaussian random variable, multiplicative displacement errors correspond to the Gaussian thermal channel via

$$\bar{n}_{\rm th} = |\alpha_b|^2 \sigma^2 \tag{S2.9}$$

where σ^2 is the variance of δ. Thus the standard deviation σ is the fractional error $|\tilde{\alpha}_b - \alpha_b|/|\alpha_b|$ of the displacement operation.

One drawback of the thermal noise model is that it treats all displacement errors equally: it assumes that amplitude errors $|\tilde{\alpha}_b| = |\alpha_b|(1 + \mathrm{Re}\,\delta)$ and phase errors $\tilde{\alpha}_b = e^{i\mathrm{Im}\,\delta}\alpha_b \approx |\alpha_b|(1 + i\mathrm{Im}\,\delta)$ have the same variance. In many settings however, the dominant error will be a phase error. Thus in what follows we also model the impact of phase errors that are Gaussian distributed. Without loss of generality we let $\alpha_b = |\alpha_b|$. The phase error is

$$\tilde{\alpha}_b = e^{i\theta}\alpha_b \approx (1+i\theta)\alpha_b \tag{S2.10}$$

where θ is a real Gaussian random variable with variance $\sigma^2 \ll 1$. We define the cavity quadratures

$$\hat{X} = \frac{1}{\sqrt{2}}(\hat{a} + \hat{a}^\dagger) \tag{S2.11}$$

$$\hat{Y} = \frac{1}{i\sqrt{2}}(\hat{a} - \hat{a}^\dagger). \tag{S2.12}$$

To linear order in θ, phase noise causes diffusion in the $\hat{Y}$ quadrature. The variance of this diffusion is $|\alpha_b|^2\sigma^2$ Thus our Gaussian phase noise model diffuses the $\hat{Y}$ quadrature such that its variance is $\langle \Delta\hat{Y}^2 \rangle = \frac{1}{2} + |\alpha_b|^2\sigma^2$ while leaving the $\hat{X}$ quadrature variance $\langle \Delta\hat{X}^2 \rangle = \frac{1}{2}$. This noise channel is easily applied to the cavity vacuum: squeeze a thermal state along the $\hat{X}$ quadrature such that the $\hat{X}$ quadrature variance is reduced to $\langle \Delta\hat{X}^2 \rangle = \frac{1}{2}$ and the $\hat{Y}$ quadrature variance is increased to $\langle \Delta\hat{Y}^2 \rangle = \frac{1}{2} + |\alpha_b|^2\sigma^2$, then perfectly displace this state by α_b. The map is

$$|0\rangle\langle 0| \mapsto \hat{D}(\alpha_b)\hat{S}(\xi)\hat{\rho}_{\mathrm{th}}(\bar{n}_{\mathrm{th}})\hat{S}^\dagger(\xi)\hat{D}^\dagger(\alpha_b) \tag{S2.13}$$

where $\hat{S}$ is the squeeze operator. The thermal occupation and squeezing are set by

$$\bar{n}_{\mathrm{th}} = \frac{1}{2}\left(\sqrt{1 + 2|\alpha_b|^2\sigma^2} - 1\right) \tag{S2.14}$$

$$\xi = \frac{1}{4}\ln\left(1 + 2|\alpha_b|^2\sigma^2\right). \tag{S2.15}$$

As was the case with the thermal noise model, applying the channel to vacuum is easy but applying it to the blockaded state is not so easy. We thus take the same approach which is to bound the second order coherence. This time, after perfectly displacing the cavity back to the origin, the output mode $\hat{c}$ is given by

$$\hat{c} = \hat{a} + \frac{i}{\sqrt{2}}dY \tag{S2.16}$$

where dY is a real Gaussian random variable with variance $|\alpha_b|^2\sigma^2$. This describes diffusion in the $\hat{Y}$ quadrature of the output mode $\hat{c}$. Assuming $\langle \hat{a} \rangle = 0$ and $\langle \hat{a}\hat{a} \rangle = 0$, the second order coherence is bounded by

$$g^{(2)}(0) \geq \frac{\langle \hat{a}^\dagger\hat{a}^\dagger\hat{a}\hat{a} \rangle}{\langle \hat{a}^\dagger\hat{a} \rangle^2} + \frac{2|\alpha_b|^2\sigma^2}{\langle \hat{a}^\dagger\hat{a} \rangle}. \tag{S2.17}$$

We compute the correlation functions in $\hat{a}$ at the end of the numerical simulation and use this expression to put a lower bound on $g^{(2)}(0)$.

Shown in Fig. S1 are numerical simulations of the time-dependent single photon generation protocol for various choices of U/κ subject to phase noise during the initial and final displacements as described above. The simulation parameters are chosen to produce (in the ideal case) a final blockaded state with $\langle 1|\hat{\rho}|1\rangle = 0.5$. The curves are labeled by the standard deviation σ of the phase noise in radians.

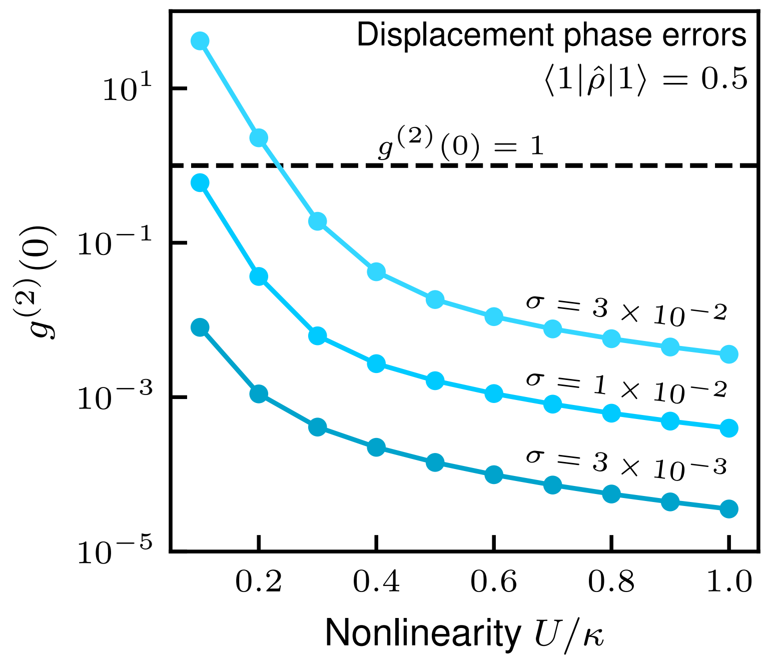

Figure S1: Numerical simulations of the performance of the single photon generation protocol in the presence of displacement phase errors during the initial/final displacement operators. Parameters are chosen such that the effective nonlinear drive amplitude $\tilde{\Lambda}_3 = 2\kappa$ and the final state has $\langle 1|\hat{\rho}|1\rangle = 0.5$. The parameter σ is the standard deviation of the phase noise in radians. Note that $g^{(2)}(0)$ must be greater than $(U/\kappa)^2\sigma^2$.